

## Some Advanced Fiber-Optic Amplitude Modulated Reflection Displacement and Refractive Index Sensors

V. Kleiza<sup>1</sup>, J. Verkelis<sup>2</sup>

<sup>1</sup>Institute of Mathematics and Informatics  
Akademijos str. 4, LT-08663 Vilnius, Lithuania  
vytautas.kleiza@ktl.mii.lt

<sup>2</sup>Semiconductor Physics Institute  
A. Goštauto str. 11, LT-01108 Vilnius, Lithuania  
jverk@pf.i.lt

**Received:** 08.12.2006    **Published online:** 05.05.2007

**Abstract.** Some advanced fiber-optic amplitude modulated reflection displacement sensors and refractive index sensors have been developed. An improved three-fiber displacement sensor has been investigated as a refractive index sensor by computer simulations in a large interval of displacement. Some new regularities have been revealed. A reflection fiber-optic displacement sensor of novel configuration, consisting of double optical-pair fibers with a definite angle between the measuring tips of fibers in the pairs has been proposed, designed, and experimentally investigated to indicate and measure the displacement and refractive index of gas and liquid water solutions. The proposed displacement sensor and refractive index sensor configuration improves the measuring sensitivity in comparison with the known measuring methods. The refractive index sensor sensitivity  $S_{n,sub} = 4 \times 10^{-7}$  RIU/mV was achieved. The displacement sensor sensitivity is  $S_{sub} = 1702$  mV/ $\mu$ m in air ( $n = 1.00027$ ).

**Keywords:** fiber-optic sensors, displacement sensors, refractive index sensor.

### 1 Introduction

Fiber-optic sensors have found many applications in recent years. Physical and chemical effects have been used to develop a variety of interferometric sensors for monitoring displacement [1], pressure [2], and other parameters [3]. One of the limitations of these sensors is that they perform well within laboratories, but in the field of applications their performance declines due to their sensitivity to vibration and temperature [4].

Intensity-modulated fiber-optic sensors have also found application [5, 6].

Fiber-optic amplitude-modulated compensated displacement sensors as refractive index sensors in [7, 8] are proposed and investigated. The light in them was launched onto the mirror through the incoming fiber, and a part of the reflected light was detected by the two outgoing fibers and photodiodes. The incoming and outgoing fibers present

in the bundle have formed an angle between them  $\theta = 0$  [7]. This configuration allows making compensated measurements [7, 8]. When measuring the ratio of outputs, the light source intensity variations, reflectivity of the mirror, opacity of the transmitting medium as well as fiber bending, light losses and influence of the temperature can be eliminated. The overall error of the refractive index  $n$  was found to be  $3 \times 10^{-3}$  [7].

Sensitivity of displacement sensors can be increased using non-parallel fiber tips distribution in the measuring head and two optical-pair fibers [9, 10]. Therefore it is interesting to investigate these sensors as refractive index sensors. The aims of this paper are:

1. To simulate the dependence of sensor's output signal  $U$  on the displacement  $h$  ( $U$ - $h$  characteristics), including the environment refractive index  $n$ , according to fiber tip distribution in [8] and to reveal their main regularities.
2. To show that it is possible to increase sensitivity of both the displacement and refractive index by creating their new configuration.

## 2 Principle of operation

Arrangement of the fiber tips, shown in Fig. 1, was applied to explain the principle of operation of the reflection fiber sensor. If the reflecting surface is a perfect mirror, the reflected light is equivalent to that transmitted from the source  $L$ , to the mirrored position  $L'$  the distance  $z$  away. According to [11], the intensity distribution function of the source  $I = I(r, z, n)$  in the position  $Q = (nr, nz)$ ,  $nr$ , and  $nz$  is an optical path on the plane  $z(h)$  away from the source and  $r$  away from the light beam axes, modified for  $n > 1$  by the authors of this paper and [12]

$$I(r, z, n) = I_0 K_0 \frac{\exp \left\{ -n^2 r^2 / R^2(z, n) \right\}}{R^2(z, n)}, \quad (1)$$

where  $I_0$  is the intensity of the light source and  $K_0$  is the loss in the intensity of the input fiber. An effective radius  $R(z, n)$  of the output optical field, is defined as

$$R(z, n) = a_0 + kz \tan \theta_c, \quad \theta_c = \arcsin(\text{NA}/n), \quad (2)$$

where  $2a_0$  is the diameter of the fiber core,  $\theta_c$  is the aperture angle of the fiber,  $k$  is the constant of the light source,  $n$  is the refractive index. We consider  $R(z, n)$  being a linear function, because of well-known linear spreading of light [9].

If the reflecting surface is not perfect and has the reflection coefficient  $K_r$ , the reflected light will be reduced by the factor  $K_r$ .

The transmitted light intensity at the end of the receiving fiber is:

$$I(r, z, n) \approx \iint_S I_0 K_r K_0 \frac{\exp \left\{ -n^2 r^2 / R^2(z, n) \right\}}{\pi R^2(z, n)} ds, \quad (3)$$

where  $K$  is the loss of the intensity of the receiving fiber, and  $s$  is the receiving fiber core area.

If the intensity at the receiving fiber center is used to represent the average intensity and the reflection coefficient of the mirror is included, then the intensity received by **A** and **B** fibers can be simplified as follows (Fig. 1):

$$A = I_A = s_1 I_0 K_r K_0 K_1 \frac{\exp \left\{ -n^2(x+d)^2 / R^2(z, n) \right\}}{\pi R^2(z, n)}, \quad (4)$$

$$B = I_B = s_2 I_0 K_r K_0 K_2 \frac{\exp \left\{ -n^2(x-d)^2 / R^2(z, n) \right\}}{\pi R^2(z, n)}, \quad (5)$$

where  $2d$  is the distance between the centers of the light receiving fibers,  $2a$  is the diameter of the fiber with cladding. In particular case  $2d$  can be equal to  $2a$ .

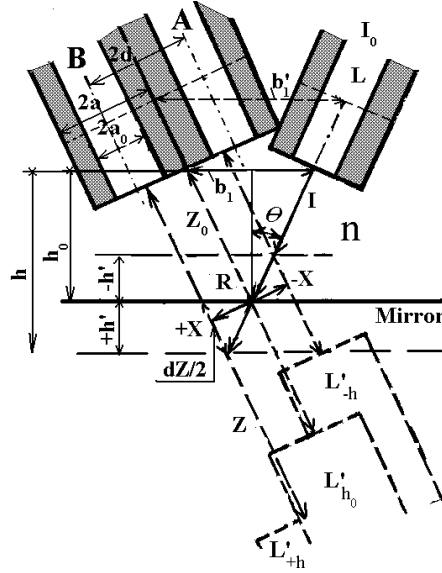


Fig. 1. Arrangement of fiber tips of the reflection fiber sensor.  $\theta$  is the angle;  $2a_0$  is the fiber core diameter,  $b_1$  is the distance between the center of a light emitting fiber and that center of two light receiving fibers;  $2d$  is the distance between the centers of light receiving fibers **A** and **B**; **L** is the position of a light emitting fiber and **L'** is the mirrored position of this fiber;  $h_0$  is the distance was signal  $A = B + h'$  and  $-h'$  is the displacement of the mirror for mirrored positions  $L'_{+h'}$  and  $L'_{-h'}$ ;  $h_0$  is the position of the mirror for  $A = B$ ;  $h$  is the position of the mirror;  $r$  is the reflection coefficient of the mirror.

When the two receiving fibers are identical,  $K_1 = K_2$ ,  $s_1 = s_2$ ,

$$\frac{(A - B)}{(A + B)} = \frac{\exp \left\{ -n^2(x+d)^2 / R^2(z, n) \right\} - \exp \left\{ -n^2(x-d)^2 / R^2(z, n) \right\}}{\exp \left\{ -n^2(x+d)^2 / R^2(z, n) \right\} + \exp \left\{ -n^2(x-d)^2 / R^2(z, n) \right\}}. \quad (6)$$

According to Fig. 1,  $x = 2h' \sin \theta$ , equation (6) is a function depending of not only on  $x$ , but also on  $z$  and  $n$ :

$$z = (z_0 + \Delta z)n, \quad z_0 = b_1 / \sin \theta, \quad \Delta z = 2h' / \cos \theta, \quad (7)$$

$$z = (b_1 / \sin \theta + 2h' / \cos \theta)n, \quad (8)$$

$z_0$  and  $h_0$  are the initial reference values when  $A = B$ , ( $U_A = U_B$ ).  $U_A - U_B = 0$  is the crossover point of the signals  $A(h)$ , and  $B(h)$ . This is the main principle of operation of the system as  $h_0 = b_1/2 \tan \theta$ ;  $h' = h - h_0$ . Function (6) can be expressed only of the function on  $h, n, \theta, \theta_c, b$  (Fig. 1).  $(A - B)/(A + B)$  does not depend on  $s_{1,2}, K_{1,2}, K_r, K_0, I_0$ . The compensation mechanism is that the signal  $(A - B)/(A + B)$  does not depend on the reflection coefficient of the mirror and intensity of the light source.

Equations (4), (5), and (6) as functions of  $h$  were used for simulation of sensors output signals in order to compare the sensitivity of our fiber constructions with those known from literature and explain the principles of their operation since the authors proposed novel sensors.

### 3 Calculation results

Output characteristics of the sensor  $U_{AB} = A$  or  $B = f(h)$ ,  $U_{sub} = (B - A) = f(h)$ ,  $U_{div} = (A - B)/(A + B) = f(h)$  for fiber tips distribution configuration presented in Fig. 1 were simulated for a different refractive index  $n$  of optical media between fiber tips and a mirror. The calculated results are plotted in Figs. 2–4 and Table 1 for different distances  $b_1 = 1.0, 1.25, 1.5, 2.0, 4.0$  mm and the angle  $2\theta = 50^\circ$ . Also, for comparison of  $b_1 = 1$  mm and  $2\theta = 5^\circ$ , between light emitting fibers and two collecting light, reflected from the mirror, all being in the plane (Fig. 1). The calculation results presented in Figs. 2–4 show that experimental characteristics [9, 10] of the sensors  $U_{AB} \sim f(h)$  and  $U_{sub} \sim f(h)$  quantitatively can be expressed by theoretical equations with Gaussian intensity distribution of the light from the emitting fiber.

The calculated output characteristics  $U_{AB} = A$  or  $B = f(h)$  are plotted in Fig. 2. The output signals  $A(h), B(h)$  rise sharply with an increase of distance  $h$  to the peak value and then decrease gradually. The segments of both at the near  $h$ -left side, and at the far  $h$ -right side of the curves  $U_{AB}(h)$  are essentially linear at the curvature points changing. Calculation was performed for three refractive index  $n$  values 1.00, 1.33, 1.41, and at the two distance values  $b_1 = 1.0, 2.5$  mm for better resolution in the pictures, and at the five distance values  $b_1 = 1.0, 1.25, 1.5, 2.0, 4.0$  mm for results represented in Table 1.

The calculation results in Fig. 2 show that the characteristics  $U_A, U_B = f(h, n)$  shifts to larger distances of  $h$  when  $b_1$  is increased and their peak values decrease. Shifted characteristics to higher values of  $h$  for  $n$  are not so large. The characteristics of signals  $U_{AB}$  cross each other at definite distances  $h_{0A,B}$  and  $h_{0n}$  for each  $n$  value (Fig. 2). The calculated characteristics  $U_{sub} = f(h)$  (Fig. 3) and  $U_{div} = f(h)$  (Fig. 4) are linear in the defined intervals of  $h$  and cross the coordinate  $h$  in the position  $h_{01.0}, h_{01.3}, h_{01.4}$  (Fig. 3 and 4) in dependent on the media  $n = 1.0, 1.3, 1.4$ . Therefore it is convenient to choose  $h_0$  as a zero position of sensors, because  $U_{sub}$  and  $U_{div}$  are applied to measurements not

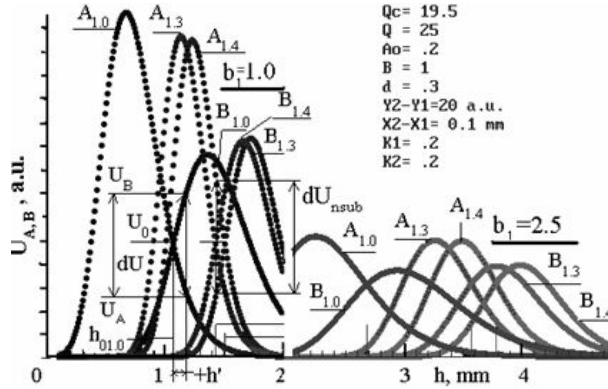


Fig. 2. Calculated  $U_{AB} = f(h)$ ,  $b_1(B) = 1$  mm,  $A, B$ .  $U_0$  is the output signal as  $U_A = U_B$ ,  $U_A - U_B = 0$ .  $\theta_c$  is the fiber aperture angle. The refractive index  $n = 1.0; 1.33; 1.41$  for curves  $A_n, B_n, (A_{10})$ .  $K_1$  and  $K_2$  are coefficients;  $dU$  is  $U_{sub}$  for change  $h_{01}$  to  $h'$ ;  $h_{01}$  is the distance for signal  $U_0$ ,  $n = 1.00$ .  $dU_{nsub}$  is the change of signal  $(A - B)$  as  $dn = 1.41 - 1.33$ .  $b_1(B) = 2.5$  m,  $A', B'$  for  $n = 1.0, 1.31, 1.41$ , respectively.

Table 1. Main calculated parameters of the sensor (Fig. 1)

Refractive index, $n$	$h_{0n}$ , mm	$S_{div}^{div} = \frac{dU_{div}}{dh}$ , ma.u./mm	$S_{sub}^{sub} = \frac{dU_{sub}}{dh}$ , a.u./mm	$S_{div}^{div} = \frac{dU_{div}}{dn}$ , ma.u./n	$S_{sub}^{sub} = \frac{dU_{sub}}{dn}$ , a.u./n	$b_1$ , mm	$S_{hn} = \frac{k}{dh/dn}$ , mm	$S_{nh} = \frac{1/k}{dn/dh}$ , mm <sup>-1</sup>	$\theta^0$
1.00	1.073	673.76	435.86	722.86	467.62				
1.33	1.43	896.18	585.97	961.48	628.67	1.0	1.072	0.9321	25
1.41	1.51	948.25	621.64	1017.34	666.94				
1.00	1.341	559.82	342.78	750.77	459.70				
1.33	1.784	749.19	462.89	1004.73	620.78	1.25	1.341	0.746	25
1.41	1.891	793.86	491.38	1064.64	658.98				
1.00	1.609	472.00	269.50	759.60	433.12				
1.33	2.140	634.41	365.48	1020.96	588.34	1.5	1.609	0.621	25
1.41	2.269	672.90	388.00	1082.92	624.43				
1.00	2.14	348.09	169.1	746.92	362.9				
1.33	2.85	470.49	231.02	1009.55	495.7	2.0	2.145	0.466	25
1.41	3.025	499.65	245.67	1072.13	527.2				
1.00	4.291	141.49	35.58	607.20	152.69				
1.33	5.708	192.89	49.46	827.82	212.23	4.0	4.291	0.233	25
1.41	6.051	205.20	52.74	880.60	226.326				
1.00	8.573	20.03	2.028	171.81	17.396				
1.33	11.40	27.38	2.834	234.84	24.310	1.5	8.577	0.117	5
1.41	12.09	29.14	3.025	249.93	25.951				

as the functions of  $h$  but that of  $h'$ . The peak values of  $\pm U_{sub}(h)$  and slopes of the curves decrease as  $b_1$  increases.  $\pm U_{div}(h)$  increases up to the value 1.000 ma. The slope of the curve  $\pm U_{div}(h)$  decreases as  $b_1$  increases (Table 1).

The refractive index sensitivity to the displacement  $S_{nh} = dn/dh$  is the constant value for a defined configuration of the sensor (Table 1), and sensitivity  $S_{nsub} = dU_{sub}/dn$  decreases as distance  $b_1$  increases (Fig. 3, Fig. 4, respectively, and Table 1). Sensitivity  $S_{ndiv} = dU_{ndiv}/dh$  reaches the peak value at  $b_1 = 1.5$  mm.

It has been determined that  $h_{0n} = h_{0nref} + (n - n_{ref})k$ , where  $h_{0n}$  is a distance for given  $n$  when the output signal  $U_{sub}, U_{div} \sim f(h) = 0$ .  $k = S_{hn} = dh/dn$  show a

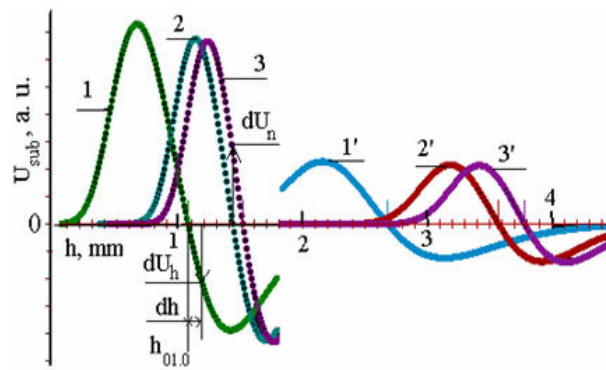


Fig. 3. Calculated dependencies for signal  $U_{sub} = (B - A)$  as  $f(h, n)$ . Curves: 1 ( $n = 1.00$ ), 2 ( $n = 1.33$ ), 3 ( $n = 1.41$ ),  $b_1 = 1.0$  mm. Curves 1', 2', 3',  $b_1 = 2.5$  mm. The main parameters of curves are in Table 1.  $dU_h$  is the signal change for  $dh$ .  $dU_n$  is the signal change for  $n = 1.41-1.33$ .  $h_{01.0}$  is the distance as  $U_{sub} = 0$  and  $n = 1.00$ .

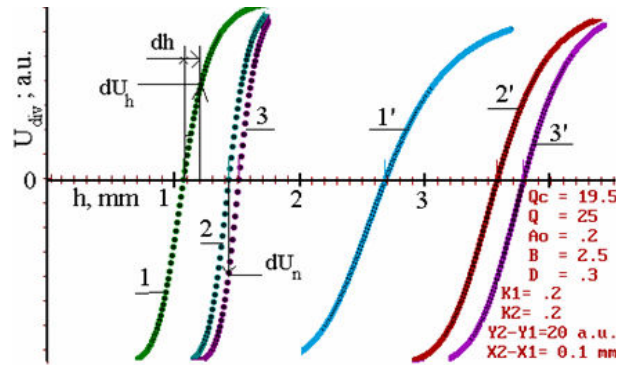


Fig. 4. Calculated dependencies  $U_{div} = (A - B)/(A + B)$  as  $f(h, n)$  for the same values of  $n$  as in Fig. 3. Curves 1, 2, 3,  $b_1 = 1$  mm. Curves 1', 2', 3',  $b_1 = 2.5$  mm.

changing distance when  $n$  is changed by 1.00. This quantity is a constant for the given sensor configuration.  $k(\theta = 25^\circ) < k(\theta = 5^\circ)$ .  $k$  increases as  $b_1$  increases (Fig. 3, Fig. 4, respectively, and Table 1).

The results of calculation presented in Table 1 have shown the sensitivity  $S_{sub} = dU_{sub}/dh$  determined in the vicinity of a small output signal to be strongly dependent on the distance  $b_1$ .  $S_{sub}$  decreases 12 fold as  $b_1$  increases from 1 mm to 4 mm.  $S_{div} = dU_{div}/dh$  decreases not so drastically, only 4.7 fold.

Sensitivity  $S_{sub}$  and  $S_{div}$  decrease more drastically as the angle  $\theta$  decreases. Table 1 has shown that  $S_{sub}$  decreases 214 fold and  $S_{div} - 33$  fold, as  $\theta = 25^\circ$  and  $\theta = 5^\circ$ .

The refraction index sensitivity  $S_{ndiv} = dU_{div}/dn$  decreases not so drastically only 1.19 fold as  $b_1$  increases from 1 mm to 4 mm.  $S_{nsub} = dU_{nsub}/dn$  decreases more sufficiently - 3.06 fold.  $S_{nsub}$  decreases 26.8 fold and  $S_{ndiv}$  decreases 4.2 fold, when the angle  $\theta$  decreases from  $25^\circ$  to  $5^\circ$  ( $b_1 = 1.5$  mm).

The constant of the defined construction of the sensor  $k = S_{hn} = dh/dn$  increases 4 fold as  $b_1$  increases from 1 mm to 4 mm and, if the angle  $\theta$  decreases from  $25^\circ$  to  $5^\circ$ , and  $k$  increases 5 fold.

Modelling results of  $U-h$  characteristics has shown that the sensitivity of the sensor can be increased by decreasing  $b_1$  as much as possible.

The main conclusion is that by adjusting parameters even of the configuration of Fig. 1, one can increase the sensor sensitivity [7, 9, 10].

However, the configuration of the sensor [8] offers some limited abilities available to optimize the characteristics of the sensor. On the grounds of our simulation of  $U(h, n)$  characteristics, we propose an advanced type of double fiber-optic-pair sensors for measuring displacement and the refractive index in cavity of the fiber tips and a mirror. This allows a more precise and effective adjustment.

The advanced new type of double fiber-optic-pair sensors has definite angles  $2\theta$  between the light emitting fiber and the fiber collecting the reflected light from a mirror in each pair as follows:  $1 - \theta_1 > \theta_2$ ;  $2 - \theta_1 = \theta_2$ .

## 4 Experimental

Experimental electronic arrangement was the same as in [10]. An additional new channel for LED intensity stabilization with a negative loop was created for measuring the output signal ( $U_A - U_B$ ). Noise of electronics did not exceed 1 mV. Experiments were carried out with fibers of a core diameter 0.4 mm. The diameter of fibers with plastic cladding was 0.8 mm and the aperture angle  $\theta_c$  was  $19.5^\circ$ . Surfaces of the fiber-tips were flat and carefully polished. Mechanic and electronic digital micrometers were used to control displacement. The whole the measuring equipment and the sensor were mounted on a laser table to reduce vibrations in an isolated laboratory with the stable humidity ( $\pm 0.5\%$ ) and temperature controlled within  $\pm 0, 2^\circ C$ . Glycerol and distilled water solutions were applied in measurements of the refractive index.

## 5 Experimental results

### 5.1 Double fiber-optic-pair sensor of the configuration ( $\theta_1 > \theta_2$ )

A new type of a fiber sensor – “double fiber-optic-pair sensor” – was proposed in [10] (Fig. 5). Two optical-pairs of fibers **A** and **B** are fixed in the holder at the distance  $d_1$  to prevent cross talking (Fig. 5(b), (c)). A mirror, one for both optical-pairs, can be positioned with respect to the fiber tips linearly by positioning the equipment and the angle with respect to fiber tips of optical-pairs and forming an angle  $\alpha$  (Fig. 5(b), (c)), or two separate mirrors for each fiber pair.

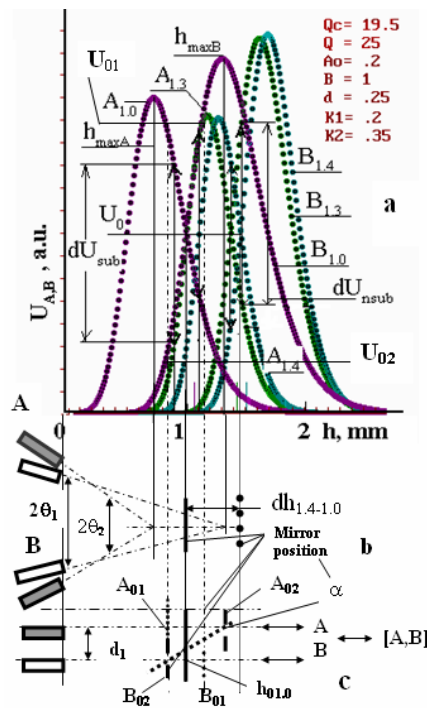


Fig. 5. (a) is the calculated  $U_{AB} = f(h, n)$ ; (b), (c) is the configuration of the sensor, (b) is a view from the top, (c) is a view from a side.

Principle of operation of the sensor is the same as in [10] and can be explained by  $U(h)$  characteristics  $A_{10}, B_{10}$  (Fig. 5(a)). Crossing of the curves can be performed by the larger factor of amplification  $K_2 > K_1$  the angle being  $2\theta_1 > 2\theta_2$  (Fig. 5(b)). Curves  $A_{10}$  and  $B_{10}$  form the crossing point with the ordinate value  $U_0$  and position  $h_{01.0}$ . In the affinity of this point, curves  $A_{10}, B_{10}$  have the larger linear intervals in comparison with three-fiber configuration. When the distance  $h_{01.0}$  is replaced by for  $-h'$ , the output signal increases to  $dU_{sub}(h')$ . The arrows on this curve represent a change in the signal. This construction of the sensor is more adjustable to obtain the operation point  $U_0$  on  $U(h)$

characteristics where the output signal  $(A - B) = 0$  (ordinate  $h_{01.0}$ , signals  $A$  and  $B$  are optimal and on quasi linear parts of characteristics for best  $S_{sub}$ ). Linearly positioning and rotating the mirror at the angle  $\alpha$ , one can obtain the crossing point amplitude  $U_{01}$  or  $U_{02}$  (Fig. 5(a) and (c)). The maximum sensitivity of the sensor  $S_{sub} = 2800 \text{ mV}/\mu\text{m}$  [10] was achieved with the crossing point amplitude  $U_{01} > U_0 > U_{02}$ . The same result can be obtained by positioning separate mirrors for optical-pairs **A** and **B** as shown in Fig. 5(c). The separate mirrors in the positions  $A_{01}, B_{01}$  represent the crossing point with the ordinate  $U_{01}$ , and  $A_{02}, B_{02}$  represent point  $U_{02}$ . After adjusting the mirror **A** and **B** is fastened, and the sensor is ready for measurements. Then both the mirrors are positioned together.

The principle of operation of the linear displacement sensor as a refractive index sensor can be explained by using the calculated  $U(h, n)$  characteristics  $A_{1.3}, A_{1.4}$  and  $B_{1.3}, B_{1.4}$  (Fig. 5(a)). The characteristics  $A_{1.3}, B_{1.3}$  with  $n$  increasing from 1.3 to 1.4 shift to larger distances  $h$  – to  $A_{1.4}, B_{1.4}$ . The output signal of the sensor increase to  $dU_{nsub}$  (Fig. 5(a)).

A novel chemical sensor (when  $\theta_1 > \theta_2$ , double fiber-optic-pair sensor) for measuring the concentration of aqua chemical solutions and the refraction index was proposed, designed, and investigated. Resolution of the refractive index sensor is  $1/S_{nsub} = dn/dU_{sub} \approx 2 \times 10^{-6} \text{ 1/mV}$ , ( $U = \pm 1 \text{ mV}$ ) and for displacement –  $S_{nh} = dn/dh = 2.5 \times 10^{-6}$ ; ( $h = \pm 1 \text{ nm}$ ), Fig. 5, Table 2. Sensitivity of the displacement sensor for  $n = 1.000$  is  $S_{disp} = dU_{sub}/dh = 1702 \text{ mV}/\mu\text{m}$  (Table 2), for the optimum configuration of the sensor fibers.

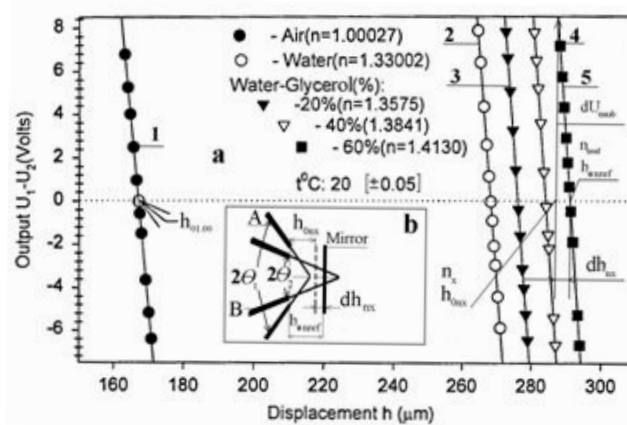


Fig. 6. (a) – experimental results of output characteristics of the refractive index sensor for signal  $U_{sub} = (B - A)$  as  $f(h, n)$  for fiber tips angle  $\theta_1 > \theta_2$  in water – glycerol solutions.  $U_1 = B$ ;  $U_2 = A$ .  $h_{01.00}$  is the value of  $h$  (as  $n = 1.00$ ); for example,  $n_{0ref} = 1.4130$ ;  $h_{0nref}$  is the value  $h$  as  $n_{0ref}$ ;  $h_{0nx}$  is the distance as  $(U_1 - U_2) = 0$  for  $n_x$ ;  $dh_{nx}$  is a change of distance as  $n_x$ . (b) is the configuration of the sensor. **A**, **B** are pairs of fibers.

Table 2. The main results from Fig. 6

Environment	$n$	$h_{0n}$ , $\mu\text{m}$	$S_{sub}$ , $\text{mV}/\mu\text{m}$	$S_{nsub}$ , $1/\text{mV}$
Air	1.00027	167.06	1702	
Glycerol % in H <sub>2</sub> O				$1.6 \times 10^{-6}$
0 %	1.3300	268.20	2085	
20 %	1.3575	267.02	2160	
40 %	1.3841	284.10	2290	
60 %	1.4130	291.60	2350	

$h_{0n}$  is the point on the  $h$  coordinate (as  $U_{nsub=0}$ ).

$h_{0nx} = h_{0nref} + (n_{0ref} - n_x)k$ ;  $k = dh/dn$ .

Dependence  $h$  of displacement characteristics on the change of the refraction index  $n$  has been experimentally evaluated as  $h = h_{0nref} + k(n - n_{0ref})$ , where the constant  $k = 306.65 \mu\text{m}/\text{RIU}$ ,  $h_{0nref}$  is the position of the mirror when  $U_{sub} = 0$  at  $n_{0ref}$  and fixed temperature, air humidity, and definite sensor configuration. This result was also predicted by simulating the characteristics  $U(h, n)$ .

The procedure of measuring  $n$  can be illustrated by the results presented in Fig. 5. For example, we must measure  $n_x$  of an unknown liquid, given  $n$  between 1.413 and 1.341.

1. For reference liquid we have the solution of  $n_{ref} = 1.4130$ . We immerse the sensor in this liquid and change the distance  $h$  between fiber tips and the mirror to obtain a zero output signal of the sensor. This distance is  $h_{ref}$ . Then we immerse the sensor in the liquid with an unknown refractive index  $n_x$ . The output signal of the sensor arises to  $dU_{sub}$ . If we have know  $S_{nsub}$  of this sensor (Table 2), we can calculate  $n_x$ .
2. When the sensor is immersed in the liquid of  $n_x$ , we change the distance  $h$ , the output signal of the sensor being zero and fix the distance  $h_{0nx}$ . If we have the constant  $k$  of the sensor, we can calculate  $n_x$ . This is a compensation method, which is useful for monitoring the fermentation process or degree of pollution.

Investigations show that, for a precise measurement of the distance  $h$ , not only temperature but also humidity must be precisely controlled or cavities must be protected by bellows.

## 5.2 Double fiber-optic-pair sensor of the configuration ( $\theta_1 = \theta_2$ )

Fundamentals of a novel prototype of the displacement and refractive index sensors  $\theta_1 = \theta_2$  were revealed designed and, manufactured (Fig. 7). This sensor has double fiber-optic-pairs. The angle  $\theta$  between the light emitting fibers and that collecting the reflected light in the pairs is  $\theta_1 = \theta_2$ . The characteristics  $A(h), B(h)$  are identical. The work point  $U_0$  at the dependence  $U_{AB} \sim f(h)$  is chosen in quasi-linear parts, as shown by the dependence  $A_{10}$  in Fig. 7. We called this principle of operation of the sensor ‘‘artificial crossing’’. In practice, it can be performed in two ways:

1. The fiber optical pairs are firmly placed in separate movable slide-blocks with the common mirror (Fig. 7(b));
2. The sensor has two mirrors on the tips of the optical-pairs in the slide-blocks. The fibers in the slide-blocks are fixed motionlessly with respect to each pair.

The first way (Fig. 7(b)) is more attractive and we shall explain it in more detail.

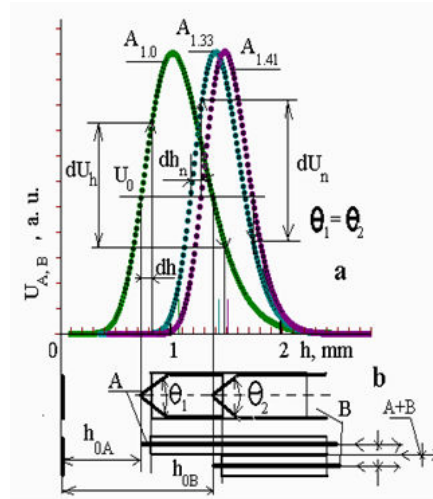


Fig. 7. (a) – calculated characteristics  $U_A \equiv U_B$  as  $f(h)$  as  $d = 0$ ;  $n = 1.00, 1.33, 1.41$  are curves  $A_{1.0}$ ;  $A_{1.33}$ , and  $A_{1.41}$  respectively.  $U_0$  is the output signal  $U_A = U_B$ .  $dU_h$  changes the output signal of the sensor as the distance of the fiber pairs from the mirror increases by  $dh$ .  $dU_n$  increases the output signal as  $n$  increases from 1.33 to 1.41.  $dh$  is a change of the distance to  $d_n$ . (b) – principle construction of the sensor  $\theta_1 = \theta_2$ . A, as well as B, are optical pairs of the fibers in sliders.  $h_{0A}$  and  $h_{0B}$  are distances of fiber tips from the mirror for each optical pair in the sliders. Arrows show adjustment of  $U_0$  to each optical-pair fiber and  $A + B$  when sliders are fixed.

By means of slide-block positioning, the distance of the fiber-optic-pair from the mirrors  $h_{0A}$  and  $h_{0B}$  is chosen so that  $U_0$  is in the quasi-linear parts of dependences  $U_A(h)$  and  $U_B(h)$ , when  $U_B(h) \equiv U_A(h)$ ,  $U_A - U_B = 0$  ( $U_0 = U_A = U_B$ ). Then the slide-blocks are fixed motionlessly with respect to each other and can move only together a distance  $dh$ . As it is seen from the characteristic  $A_1$ , which, in this case, is identical to the characteristic  $B_1$  (Fig. 6(a)), when increasing the distances  $h_{0A}$  and  $h_{0B}$  by  $(+dh)$ , the output signal  $(U_A - U_B)$  increase from 0 to  $dU_{h(sub)}$ . This is the maximum signal for obtaining a possible displacement using  $U_{AB} \sim f(h)$  dependences by equally amplifying the electronic channels A and B. When the refractive index of the media between the mirror and the fiber tips in this system is changed from 1.3 to 1.4, the dependence  $A_{1,3}$  changes to  $A_{1,4}$ . Then the signal  $U_A - U_B$  increases from 0 to  $dU_{n(sub)}$  ( $A \equiv B$ ) (Fig. 7(a)). Meanwhile, in the scheme of fiber tips distribution

presented in Fig. 1, the signal increases only by  $dU_{sub}(\theta)$  or  $dU_{nsub}, dU_{ndiv}$  (Fig. 3, 4). The experimental investigation has shown that the sensitivity  $S_{nsub}$  of this refractive index sensor is highest. As the theoretical investigation shows,  $S_{ndiv} = dU_{div}/dn$  does not depend on the reflection coefficient changes of the mirror as well as on ageing of the light source and its fluctuations. With an increase of  $b_1$ ,  $S_{nsub}$  decreases and  $S_{ndiv}$  increases in the same way, as Table 1 shows for the configuration in Fig. 1. These constructions may be used to measure refraction indices of liquids and concentrations of salts in water solutions, at fixed  $h_{0nref}$  ( $n_{0ref}$ ), by measuring the calibrated  $U_{nsub}$  and  $U_{ndiv}$  signal values of the sensor, as well as by the compensation method  $U_{nsub} = 0$  and  $U_{ndiv} = 0$  and measuring calibrated position  $h_{0nx}$  (Fig. 7),  $S_{nh} = (h_{0nx} - h_{0nref})/(n_x - n_{0ref})$ ,  $n_{0ref}$  where is a reference liquid refractive index. The sensitivity to the change of the refractive index is  $1/S_{nsub} = 4 \times 10^{-7}$  RIU/mV for the prototypes in Fig. 7(b) ( $A \equiv B$ ). The temperature and humidity conditions were fixed the same as for the sensor  $\theta_1 > \theta_2$ .

## 6 Conclusions

The advanced double fiber-optic-pair reflection sensor has been proposed for measuring displacement, refractive index and concentration of liquid solutions.

$U(h, n)$  characteristics of the displacement sensor, proposed and investigated in [10] in a narrow interval of  $h$ , were calculated by improved theoretical relations in real media with the refractive index  $n$  in a wider interval of  $h$ , and fundamental regularities have been revealed.

Advanced in sensitivity, new types of double fiber-optic-pair sensors  $\theta_1 = \theta_2$  and  $\theta_1 > \theta_2$  have been proposed and principles of operation revealed and explained by the results of the  $U(h)$  calculations. The best sensitivity to displacement and refractive index measurements has the  $\theta_1 = \theta_2$  sensor operation principle based on creating of “artificial crossing” of the  $U-h$  characteristics of the fiber-optic-pairs in comparison with the type of sensors in [10]. A universal and easily adjustable to maximum sensitivity sensor has been developed for measuring displacement and therefore refractive index. The main difference of the double fiber-optic-pair displacement sensors from the refractive index sensor is that the latter has a firmly fixed mirror relative to fixing fiber tips and forming the construction. The sensors have all the merits of earlier prototypes [7, 8, 11] to compensate automatically the changes in light source intensity, reflectivity of the mirror, and due temperature. The developed fiber-optic sensors can be applied in creating optical devices: dilatometers, dynamometers, torque devices as well as the pressure and gas devices for automated monitoring of pollution and for fermentation.

## References

1. T. Wang, S. Zheng, Z. Yang, A high precision displacement sensor using a low finesse fiber-optic Fabry-Perot interferometer, *Sensors and Actuators A*, **69**, pp. 134–138, 1998.
2. X.Z. Tu, J.N. Zemel, Vertical membrane optical-fiber pressure sensor, *Sensors and Actuators A*, **39**, pp. 49–54, 1993.

3. S. Mc Murtry, J. D. Wright, D. A. Jackson, A multiplexed low coherence interferometric system for humidity sensing, *Sensors and Actuators B*, **67**, pp. 52–56, 2000.
4. A. J. Zuckerwar, F. W. Cuomo, T. D. Nguyen, S. A. Rizzi, S. A. Clevenson, High-temperature fiber-optic lever microphone, *J. Acust. Soc. Am.*, **97**(6), pp. 3605–3616, 1995.
5. H. Golbani, Fiberoptic displacement sensor using a coated lens optic, *Rev. Sci. Instruments*, **71**, pp. 4314–4318, 2000.
6. A. Paritsky, A. Kots, *Sensor and method for measurement distance to and/or physical properties of a medium*, US Patent Nr.6 239 865, 2001.
7. A. Suhadolnik, A. Babnik, J. Mozhina, Optical fiber reflection refractive index sensor, *Sensors and Actuators B*, **29**, pp. 428–432, 1995.
8. W.H. Ko, K.-M. Chang, G.-I. Hwang, A fiber-optic reflective displacement micrometer, *Sensors and Actuators A*, **49**, pp. 51–55, 1995.
9. J. Verkelis, R. Jankevicius, R. Sarmaitis, Advanced fiber-optical angular and linear displacement sensors and refractive index sensors, in: *Proc. of the 14th European Conf. on Solid-State Transducers "Euroensors XIV"*, Copenhagen, Aug. 27–30, 2000, pp. 565–568, 2000.
10. J. Verkelis, R. Jankevicius, R. Sarmaitis, *Lithuanian Journal of Physics*, **43**(2), pp. 99–109, 2002.
11. Y. Libo, P. Jian, Y. Tao, H. Gouchen, Analysis of fiber-optic displacement sensor, *Sensors and Actuators A*, **36**, pp. 177–182, 1993.
12. M. Born, E. Wolf, *Principles of Optics*, Pergamon, New York, 1975.
13. J. Verkelis, V. Dikinis, R. Sarmaitis, Fiber-optic reflection displacement sensor, in: *Proc. of the 12th European Conf. on Solid-State Transducers and the 9th UK Conf. on Sensors and their Applications "Euroensors XII"*, Southampton, Sept. 13–16, 1998, pp. 315–318, 1998.